

Chapter 1. Global agroclimatic patterns

Chapter 1 describes the CropWatch Agroclimatic Indicators (CWAIs) rainfall (RAIN), temperature (TEMP), and radiation (RADPAR), along with the agronomic indicator for potential biomass (BIOMSS) in sixty-five global Monitoring and Reporting Units (MRU). RAIN, TEMP, RADPAR and BIOMSS are compared to their average value for the same period over the last fifteen years (called the “average”). Indicator values for all MRUs are included in Annex A table A.1. For more information about the MRUs and indicators, please see Annex B and online CropWatch resources at www.cropwatch.com.cn.

1.1 CropWatch agro-climatic indicators (CWAIs)

This bulletin describes environmental over the period from April to July 2019, AMJJ, referred to as “reporting period”. In this chapter, we focus on 65 spatial “Mapping and Reporting Units” (MRU) which cover the globe, but CWAIs are averages of climatic variables over agricultural areas only inside each MRU. For instance, in the “Sahara to Afghan desert” MRU, only the Nile valley and other cropped areas are considered. MRUs are listed in annex B and serve the purpose of identifying global climatic patterns. Refer to Annex A for definitions and to table A.1 for 2019 AMJJ numeric values of CWAIs by MRU).

Although they are expressed in the same units as the corresponding climatological variables, CWAIs are spatial averages limited to agricultural land and weighted by the agricultural production potential inside each area.

We also stress that the reference period, referred to as “average” in this bulletin covers the 15 year period from 2004 to 2018. Although departures from the 2004-2018 are not anomalies (which, strictly, refer to a “normal period” of 30 years), we nevertheless use that terminology. The specific reason why CropWatch refers to the most recent 15 years is our focus on agriculture, as already mentioned in the previous paragraph. 15 years is deemed an acceptable compromise between climatological significance and agricultural significance: agriculture responds much faster to persistent climate variability than 30 years, which is a full generation. For “biological” (agronomic) indicators used in subsequent chapters we adopt an even shorter reference period of 5 years (i.e. 2014-2018) but the BIOMSS indicator is nevertheless compared against the longer 15YA (fifteen years average). This makes provision for the fast response of markets to changes in supply but also to the fact that in spite of the long warming trend, some recent years (e.g. 2008 or 2010-13) were below the trend.

Correlations between variables (RAIN, TMP, RADPAR and BIOMSS) at MRU scale derive directly from climatology. For instance, the positive correlation ($R=0.322$) between rainfall and temperature results from high rainfall in equatorial, i.e. in warm areas.

Considering the size of the areas covered in this section, even small departures may have dramatic effects on vegetation and agriculture due to the within zone spatial variability of weather.

It is important to note that the current bulletin adopts a new definition and calculation procedure of the biomass production potential. Previous bulletins based BIOMSS on TEMP and RAIN, considering that both variables have a beneficial impact on biomass accumulation, following a saturation type curve, i.e. a sigmoid starting a low values and reaching a plateau at higher values. The new methodology is sounder from a physiological point of view: it considers that the main factor in plant production is sunshine, but that solar energy used for photosynthesis can actually be “absorbed” only if sufficient water is available. The approach, known as “the Chikugo model” [1] was adapted to Monitoring by CropWatch: we first compare sunshine (RADPAR) with available water (RAIN) and estimate how much solar energy E can be

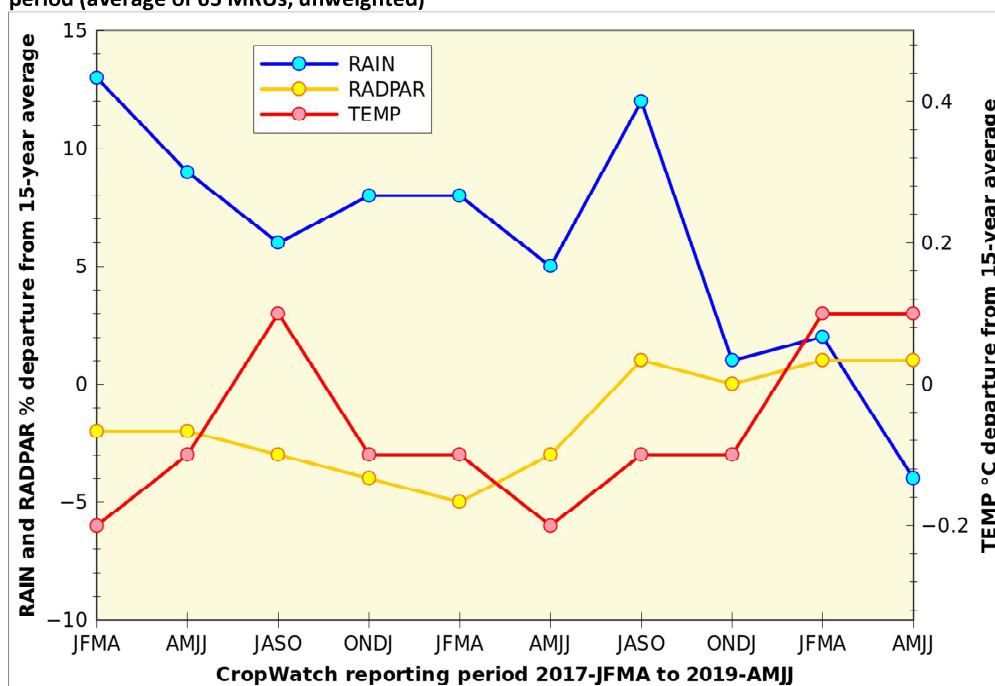
converted to chemical energy in plant biomass. The result is then multiplied by a temperature function (a sigmoid) that reduces at low temperature. In the new biomass accumulation potential calculation procedure, BIOMSS thus depends no longer on two (RAIN, TEMP) variables but on three: RAIN, TEMP and particularly RADPAR.

1.2 Global agro-climatic overview

The current reporting period was dominated by large temperature anomalies worldwide, which received wide media coverage. According to WMO and other national sources (see sources [2] to [4] at the end of the chapter) June was the hottest June on record, and July was not only the hottest July on record but also the hottest month ever recorded on the planet. According to the source of data and calculation procedures, the global temperature anomaly for AMJJ against 2004-2018 reached between 0.2°C and 0.4°C.

RAIN was above average only in one third of the MRUs (31%), resulting in RAIN 4% below the average value of the 15-year reference period (2004-2018) over agricultural areas. It is striking (Figure 1.1) that quarterly AMJJ precipitation has been on a downward trend over the last two years, paralleled by increasing temperature and sunshine.

Figure 1.1. Global departure from recent 15 year average of the RAIN, TEMP and RADPAR indicators since 2017 AMJJ period (average of 65 MRUs, unweighted)



RADPAR was above average in the majority of MRUs (44 out of 65, or 68%) resulting in a slightly above average value of 1%. Because MRUs are large areas, and because sunshine tends to be less variable than rainfall and temperature, the 1% departure for RADPAR is more significant than it would be for rain.

For the agricultural areas monitored by CropWatch, TEMP was minimally above average (average departure +0.1°C) with 58% of MRU with positive anomalies; TEMP anomaly was the most variable agro-climatic factor with the coefficient of variation reaching 816% (in comparison to 603% for RAIN anomaly and 250% for both RADPAR and BIOMSS anomalies). Finally, BIOMSS exceeds the average in 63% of MRUs resulting in the second largest average departure of +3%. The BIOMSS departures from the

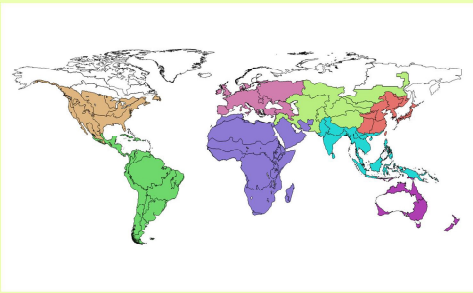
average displays the strongest correlations with TEMP departures ($R=0.451$) and PAR departures ($R=0.356$). Altogether, about half the anomalies in the biomass production potential are explained by the anomalies in TEMP, RAIN and RADPAR, about one third each.

When MRU average departures are computed using agricultural area as a weighting factor, a positive rainfall departure of 1% is observed (Table 1.1). For the other variables, the weighting does not affect the magnitude of the departures.

During the current AMJJ reporting period, global departure from average patterns tend to be largely independent of the individual variables values (i.e. RAIN with RAIN departure, TEMP with TEMP departure etc.), indicating that there is little zonality in anomalies.

Table 1.1. Departures from the recent 15-year average of CropWatch agro-climatic indicators over regional MRU groups. Within each group, averages are weighted by the agricultural area of individual MRUs. "Others" include five nonagricultural areas shown in white in the map. They are located mostly at high northern latitudes.

	RAIN %	TEMP °C	RADPAR %	BIOMSS %
Africa	3	0.0	2	5
America S + C	-3	0.3	1	3
America N	19	-0.6	-1	-2
Asia centre	20	-0.4	0	1
Asia East	-12	0.1	-1	-2
Asia South	-13	0.3	4	6
Europe	-4	0.0	2	4
Oceania	-30	0.3	4	-1
Others	-21	0.7	4	9
World	0.9	0.0	1.3	2.4



On a continental basis, RAIN anomalies were largest in North America (+20% above average), central Asia (+19%) and in Oceania (-30%). The largest positive TEMP anomalies over agricultural areas occurred in south Asia and Oceania and were both mentioned in the section on disasters. The most significant cold waves affected North America (-0.6°C) and central Asia (-0.4°C) and were accompanied by abundant precipitation, as mentioned. Significant and positive sunshine anomalies occurred in south Asia and in Oceania, both at +4%. Finally, positive biomass anomalies due to sunshine (RADPAR) brought about high rainfall or favorable sunshine conditions occurred in Africa and southern Asia.

1.3 Rainfall

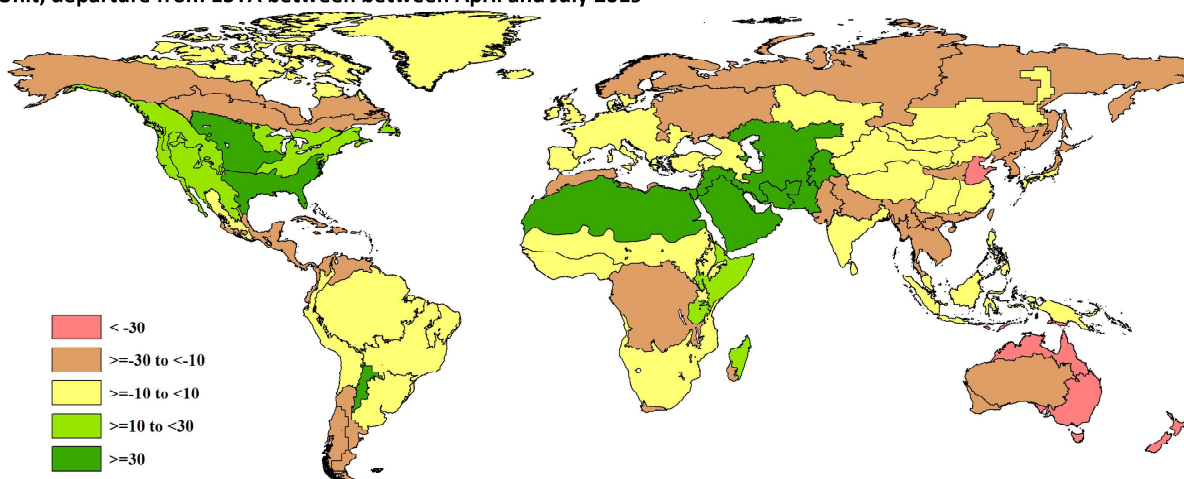
A. Dry conditions

Apart from Boreal areas in Europe and America, which are of limited agricultural importance, the driest areas were generally associated with high temperature and high sunshine. They occurred mainly in Oceania and on the eastern fringe of the Asian continent. MRU34 (Huanghuaihai, -50% compared with average) was the driest MRU in absolute. Neighboring areas are in the range from -20% to -23% and include MRU42 (Taiwan), MRU43 (East Asia) and MRU50 (Mainland Southeast Asia). While Maritime

South-East Asia (MRU49) had a moderate deficit of 9%, higher values in the range from -34% to -31% occur again in northern Australia (MRU53), Queensland to Victoria (MRU54) and New Zealand (MRU56).

The driest areas in Africa comprise of MRU06 (Southwest Madagascar, -24%) and MRU10 (Western Cape, -23%) do not raise concern because they are not currently in the main cropping seasons. Several South American MRUs, on the other hand, are in the summer/rainy season. Range-land is likely to have suffered in MRU27 (Western Patagonia, -23%) and the MRU28 Semi-arid Southern Cone (MRU28, -27%). At the other end of Latin America, dry conditions prevailed as well in Central America and especially in the Caribbean (MRU20) where the precipitation shortfall reached -27%.

Figure 1.2. Global map of rainfall anomaly (as indicated by the RAIN indicator) by CropWatch Mapping and Reporting Unit, departure from 15YA between between April and July 2019



B. Wet conditions

The largest area with consistently high rainfall occurred in northern America, involving especially the Cotton Belt to the Mexican Nordeste (MRU14, +30%) and the Northern Great Plains where MRU12 recorded a precipitation excess of 33%. Excesses between 12% and 20% occurred in the south-western U.S.A and the north Mexican highlands (MRU18, +12%), the Corn Belt and the area from British Columbia to Colorado (MRUs 13 and 11) as well as the West Coast (MRU16)

Sometimes significantly larger excesses were recorded, among others over central and northern Madagascar (MRU05, +17%) resulting from cyclone Kenneth (refer to Chapter 5.2), the Horn of Africa (MRU04, +26%) and especially Sahara to Afghan deserts (MRU64, +89%, i.e. 47 mm instead of 25 mm).

Abundant rainfall occurred in western Asia east of The Sahara to Afghan deserts MRU, in the MRUs of the Pamir (MRU30, +44%) and in MRU31 (+50%)

In south America, it is necessary to mention only MRU25 (Central-north Argentina) with precipitation up 43% compared with average.

1.4 Temperature

C. Below average temperature

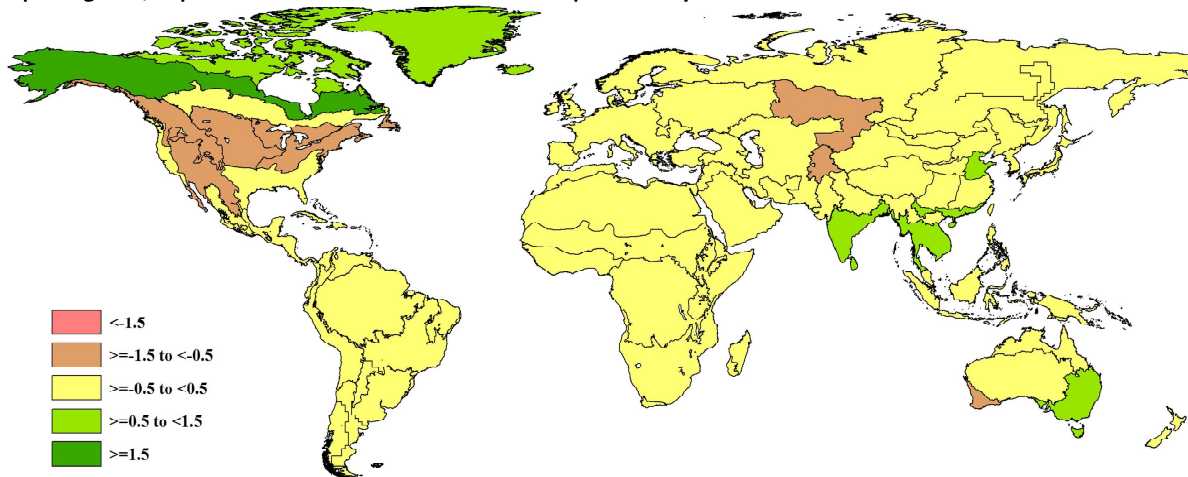
Cool to relatively cold weather prevailed in most of the areas affected by excess precipitation in north America in MRU18 (South-western USA and the northern Mexican highlands, -0.6°C compared with average), MRU11 and 13 (British Columbia to Colorado and the Corn Belt, both at -0.5°C) and especially in the Northern Great Plains (MRU12) where temperature was more than 1°C below average (1.3°C).

Central western Asia recorded cool weather 0.8°C below average in MRU62 (Ural to Altai Mountains) and in the already mentioned Pamir area (MRU30) where precipitation was larger than average.

D. Above average temperature

In addition to the south-American Pampas (MRU26) many areas in southern and eastern Asia recorded temperature exceeding average by values between 0.5°C and 1.0°C , including MRU34 (Huanghuaihai), MRU42 and MRU33 (Taiwan and Hainan), MRU40 (Southern China), MRU50 (the south-eastern Asian Mainland). MRU54 (Queensland to Victoria) also recorded an excess of 0.6°C .

Figure 1.3. Global map of temperature anomaly (as indicated by the TEMP indicator) by CropWatch Mapping and Reporting Unit, departure from 15YA between April and July 2019



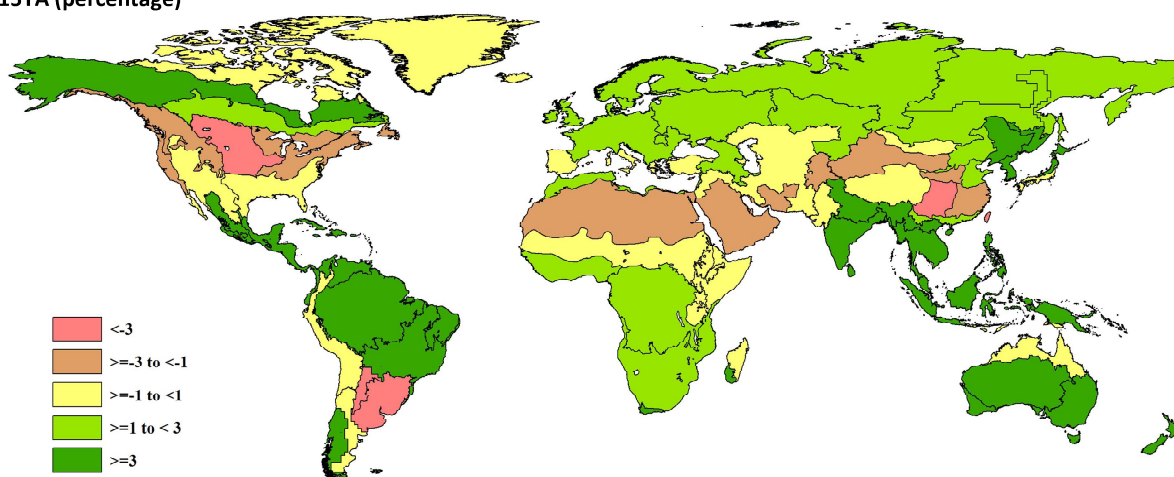
1.5 RADPAR

Several of the areas listed above with warm weather also experienced correlated sunny weather, especially southern China (MRU33, Hainan, +10%), MRU50 (Mainland Southeast Asia, +8%), New Zealand (MRU56, +7%) as well as parts of Australia (e.g. MRU55, Nullarbor to Darling, +5 %.)

Sunshine departures of similar magnitude were also recorded in MRU22, the Brazilian Nordeste.

The negative sunshine departure that accompanied low temperature and abundant precipitation in the Northern Great Plains (MRU12) was relatively modest at 3%. More significant sunshine deficits with a potential negative crop and range-land impact include the South American Pampas (MRU 26, -6%) and MRU25 (Central-north Argentina) where the RADPAR drop reaches -9%, the absolute record for the current reporting period. This is followed immediately by MRU41 (Southwest China) with a drop of 7%.

Figure 1.4. Global map of April - July 2019 PAR anomaly (as indicated by the RADPAR indicator) by MRU, departure from 15YA (percentage)



1.6 BIOMSS

The new calculation procedure for the BIOMASS indicator incorporates the combined effect of precipitation, sunshine and temperature. It is a very synthetic climate-based but agronomic value-added indicator which assesses the biomass production potential and hence the likely effect of weather on crop photosynthesis.

The record low values are assessed for MRU12, the Northern Great Plains, with an 8% drop in the biomass production potential. A production loss of the same magnitude is projected for MRU25, Central-north Argentina, where range-land and livestock production play a more important part than crop husbandry. The Mexican Sierra Madre (MRU17) is expected to lose 5% of biomass production compared to average.

Outside of the American continent, negative weather impact is likely to result in a 7% loss in Southwest China (MRU41) and a 6% drop in Northern Australia (MRU53). MRU20 (Caribbean) and MRU 22, the Brazilian Nordeste are expected to increase production by 5% and 7%, respectively) mostly due to favorable sunshine under conditions of sufficient water supply, even if RAIN was down 27% in MRU20.

In Asia, both MRU47 (Southern Mongolia) and MRU33 (Hainan) underwent a BIOMSS increase of 9%. The increase reaches 6% in MRU50 (Continental Southeast Asia). A huge contiguous area extending from the South China Sea to western Asia includes three MRUs (44, 48, and 31) where the BIOMSS reaches 9% (Southern Himalayas), 11% (Punjab to Gujarat) and 7% in Western Asia. Just across the Black Sea from the previous area, non-Mediterranean Western Europe (MRU60) experienced a rise of 6% in BIOMSS covering the final stages of winter crops and early stages of summer crops. The rise mostly results from RADPAR up 2% in a region where low radiation tends to limit crop production.

In New Zealand (MRU56) relatively warm winter conditions associated with favorable sunshine have pushed up BIOMSS by 7%.

The remaining areas that deserve mentioning are located in Africa. They include the two MRUs of Madagascar (MRU05, the central and northern half of the Island, and MRU06, the semi-arid south-west). BIOMSS is up 9% and a spectacular 27%, respectively. The increase will benefit off-season biomass: range land in MRU06 and late planted main-season crops elsewhere. Of the two adjacent areas of the Sahel (MRU08, +9%) and MRU64 (Sahara to Afghan deserts) the second benefited from a huge BIOMSS increase of 30% resulting from a large increment in precipitation combined with a decrease in RADPAR, which reduced water demand. The increase in the Sahara to Afghan deserts has benefited pastures while in the Sahel; the rain may have favored early planting.

Figure 1.5. Global map of biomass production potential anomaly (as indicated by the BIOMSS indicator) by CropWatch Mapping and Reporting Unit, departure from 15YA between April and July 2019

